Fabrication and Functionalization of Dendritic Poly(amidoamine)−Immobilized Magnetic Polymer Composite Microspheres

ARTICLE *in* THE JOURNAL OF PHYSICAL CHEMISTRY B · APRIL 2008

Impact Factor: 3.3 · DOI: 10.1021/jp077465x · Source: PubMed

Fabrication and Functionalization of Dendritic Poly(amidoamine)-Immobilized Magnetic Polymer Composite Microspheres

Hongbo Liu,† Jia Guo,† Lan Jin, Wuli Yang, and Changchun Wang*

Key Laboratory of Molecular Engineering of Polymers (Ministry of Education) and Department of Macromolecular Science and Advanced Materials Laboratory, Fudan University, Shanghai, China 200433

Received: September 17, 2007; In Final Form: December 26, 2007

The synthesis of functionalized magnetic polymer microspheres was described by a process involving (1) preparation of the monodisperse magnetic seeds according to a two-step procedure including the preparation of bilayer-oleic acid-coated Fe_3O_4 nanoparticles followed by soap-free emulsion polymerization with methyl methacrylate (MMA) and divinyl benzene (a cross-linking agent, DVB); (2) seeded emulsion polymerization proceeding under the continuous addition of glycidyl methacrylate (GMA) monomers in the presence of the magnetic PMMA seeds; and (3) chemical modification of the PGMA shells with ethylenediamine (EDA) to yield amino groups. As such, the magnetic poly(MMA-DVB-GMA) microspheres were prepared possessing monodispersity, uniform magnetic properties, and abundant surface amino groups. Then, the dendritic poly(amidoamine) (PAMAM) shells were coated on the magnetic particles on the basis of the Michael addition of methyl acrylate and the amidation of the resulting ester with a large excess of EDA, which could achieve generational growth under such uniform stepwise reactions. For improving the luminescence properties of the composite particles, fluorescein isothiocyanate, which is a popular organic dye, was reacted with the terminal -NH_2 groups from the dendritic PAMAM shells, resulting in the formation of multifunctional microspheres with excellent photoluminescence, superparamagnetic, and pH-sensitive properties. In this case, it can be expected that an extension of the functionalization of these microspheres is to immobilize other target molecules onto the PAMAM shells to introduce other desired functions for potential chemical and biological applications.

1. Introduction

Magnetic nanoparticles have been studied extensively for various biological applications such as magnetic resonance imaging,[1] drug delivery,[2] magnetofection,[3] biotechnology/biomedicine,[4,5] and magneto-thermal therapy.[6] For these applications, the surfaces of these particles were modified through the creation of a few atomic layers of organic polymers or inorganic metallic or oxide surfaces, suitable for further functionalization by the attachment of various bioactive molecules.[7] However, note that such small particles not only tend to form agglomerates to reduce energy but also show themselves to be chemically highly active, resulting generally in a loss of magnetism and dispersibility. One of the main reasons is their intrinsic instability in the physiological environment as well as association with nanosized ranges.[8] As a result, it is crucial to develop protection strategies to chemically stabilize the magnetic nanoparticles against degradation or aggregation. Among these methods, it has been well-established that the embedding of iron oxide nanoparticles within polymeric matrices prevents their aggregation in physiological media and preserves their physicochemical properties. However, polymeric magnetic particles have difficulty in producing a high density of functional groups for the coupling of affinity ligands or the binding of biomolecules. Up to now, surface functional groups usually are introduced into magnetic polymer particles by two main methods, namely, copolymerization and chemical modification of the preformed polymer. In copolymerization, a large amount of functional groups is usually buried in the polymer, and only a low surface density of functional groups is obtained.[9] Chemical modification has been reported to be an efficient way to obtain abundant functional groups on the magnetic particles.[10] However, the achievement of surface functional groups is restricted by the polymer nature and incomplete heterogeneous reactions. As a result, there is a need to find new strategies for improving the population of functional groups.

Poly(amidoamine) (PAMAM) dendrimers are hyper-branched synthetic macromolecules with highly controllable sizes and abundant terminal groups on the basis of uniform stepwise reactions used to achieve generational growth. Generally, solution-phase synthesis of dendrimers is often challenging, requiring a long reaction time and nontrivial purification. Solid-phase methodology, on the other hand, as outlined by Merrifield et al.,[11,12] enabled reactions to be driven to completion by using a large excess of reagents with simple and trivial purification. In recent years, dendrimers grown on solid materials such as polymer beads,[13,14] magnetite nanoparticles,[15] carbon black,[16] and silica[17−19] have attracted much interest for the design of innovative dendritic materials for a variety of advanced applications. Particularly in medicine and diagnostics, substantial progress achieved in several groups has led to a burst of activity on the generation of dendrimer-immobilized nanoparticles as biosenosors.[15,20] As a result, if the solid supports as initiator cores can be functionalized for the immobilization of the PAMAM dendrimers, these dendrimer-based solid supports will be of a core−shell type: functionalized cores and dendrimer

* Corresponding author. Tel.: 86-21-65642385; fax: 86-21-65640291; e-mail: ccwang@fudan.edu.cn.

† These authors contributed equally to this work.

10.1021/jp077465x CCC: $40.75
Published on Web 02/19/2008

SCHEME 1: Schematic Illustration of Preparation of Dendritic PAMAM-Immobilized Magnetic Poly(MMA-DVB-GMA) Microspheres with Coupling of FITC

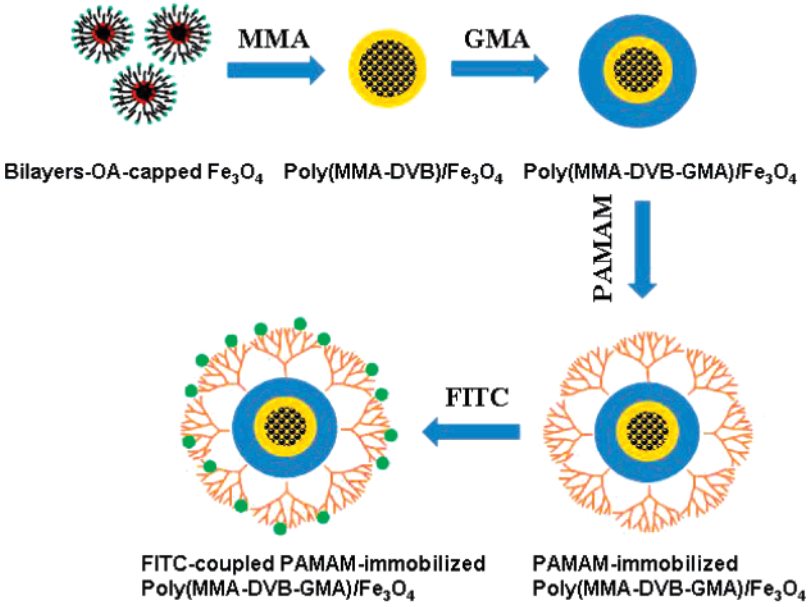

shell coupling biological active molecules at the periphery for the recognition of specific biomolecules. This will be another novel strategy for the development of different biomedical technologies based on PAMAM dendrimers.

In this paper, we present a flexible and robust approach to prepare dendritic PAMAM-grafted magnetic polymer microspheres with the coupling of fluorescence probes. As shown in Scheme 1, first the cross-linked magnetic poly(methyl methacrylate) (PMMA) composite latexes were prepared using soap-free emulsion polymerization in the presence of bilayer-oleic acid (OA)-coated magnetite nanoparticles. For achieving the functionalized particle surfaces, the polymerization of glycidyl methacrylate (GMA) in the presence of magnetic PMMA seed particles using the continuous addition of GMA can form magnetic PMMA/PGMA latex particles with a well-defined core−shell structure containing a magnetic PMMA core and PGMA shell. And thus, PAMAM dendrimers may be synthesized conveniently and efficiently on such magnetic supports after chemical modification of the PGMA shell with ethlenediamine (EDA) to yield amino groups. The as-synthesized PAMAM dendrimers for modifying the microspheres are based on repetitive reaction sequences, which were comprised of the Michael addition of methyl acrylate (MA) and condensation (amidation) of the resulting ester with large excesses of EDA, leading to each successive generation. Thus, the surface amino groups can be used for the attachment of various functional molecules, for example, targeting agents, imaging agents, and therapeutic drugs. Fluorescein isothiocyanate (FITC), which is a popular fluorescence probe, has been chemically bonded to the -NH_2-terminated PAMAM shells, creating FITC-coupled magnetic PAMAM-immobilized microspheres. Additionally, another motivation of this work was to produce multifunctional microspheres with the following desired functionality in the targeted drug delivery: (1) due to the primary amino groups present on the surface, pH-responsive PAMAM dendrimers can be used as nonspecifically targeted controlled drug delivery systems triggered at low pH; (2) the magnetite nanoparticles allow the manipulation of these drug carriers by an external magnetic field toward the caner sites; (3) FITC molecules coupled on the PAMAM surface allow the tracing of drug delivery by fluorescence spectroscopy in complicated systems. On the basis of the previous considerations, these microspheres could be used as models to study the basic process of controlled delivery systems for drugs as well as other related biomedical fields.

2. Experimental Procedures

2.1. Materials. Potassium persulfate (KPS; Shanghai Chemical Reagent Co.) was recrystallized from deionized (DDI) water. MMA (Shanghai Chemical Reagent Co.) and GMA (Aldrich) were purified by distillation under reduced pressure. DVB (55% grade, balance between *m*- and *p*-ethylstyrene) was dehibited by being passed over a column of activated neutral alumina. MA (CP), EDA (CP), and methanol (AP) were purchased from Shanghai Chemical Reagent Co. and used as received. FITC was purchased from Aldrich and used as received.

2.2. Synthesis of Bilayer-OA-Coated Fe_3O_4 Nanoparticles. The Fe_3O_4 nanopariticles were synthesized by coprecipitation of Fe (II) and Fe (III) salts. In a typical procedure, an aqueous solution of 0.86 g of $FeCl_2 \cdot 4H_2O$ and 2.35 g of $FeCl_3 \cdot 6H_2O$ was charged in a 100 mL four-necked round-bottomed flask that was equipped with a Teflon blade mechanical stirrer and a nitrogen inlet. After the solution was heated to 80 °C with stirring for 30 min under a stream of nitrogen, 100 mg of oleic acid dissolved in 5 mL of acetone was added to the flask, and then 10 mL of ammonia solution (25−28 wt %) was added. Ten minutes later, 1 g of oleic acid was added dropwise within 30 min. After heating for another 30 min, the magnetic particles were precipitated by dropwise addition of a 2 M HCl solution and then washed with acetone 5 times to remove the excessive oleic acid. A total of 30 mL of the ammonia solution (0.16−0.18 wt %) and 1 g of oleic acid were added to disperse the magnetic precipitates, and then the solution was bubbled with nitrogen and heated to 80 °C for 30 min. Finally, the magnetic fluids were stored in nitrogen atmosphere for further use.

2.3. Synthesis of Magnetic Poly(MMA-DVB-GMA) Microspheres. *2.3.1. Magnetic Particles as Seeds.* Poly(MMA-DVB)/Fe_3O_4 seed particles were prepared by batch soap-free emulsion polymerization at 70 °C for 24 h using 3 g of magnetic fluids (3.3 wt %), 1.35 g of MMA, 0.15 g of DVB, 0.045 g of KPS, and 45.5 g of H_2O. The resulting products were placed

on the magnet for 30 min and subsequently collected as seeds for further polymerization of GMA monomers.

2.3.2. Poly(MMA-DVB-GMA)/(MMA-DVB)/Fe_3O_4 Microspheres. In a typical procedure, 0.1 g of magnetic seeds and 44.4 g of H_2O were charged in a four-necked round-bottomed flask and then heated to 70 °C with stirring under a stream of nitrogen. A total of 0.01 g of KPS as initiators was introduced, and then the polymerization was conducted by dropwise addition of the mixed monomers (0.25 g of GMA, 0.20 g of MMA, and 0.05 g of DVB) at a speed of 1 mL h^{-1}. After 12 h of polymerization, the product was washed with water 3 times by magnetic separation.

2.4. Preparation of Dendritic PAMAM-Modified Magnetic Polymer Particles. The dendritic polymer shell on the surface of the particles was prepared according to the dendritic PAMAM synthesized procedure,[16] which involved reiterative two-step reaction sequences. These sequences consist of (1) an exhaustive alkylation of primary amines (Michael addition) and (2) amidation of the ester group.

Michael addition was carried out as follows: 50 mL of a methanol solution of MA (2 equiv of amino groups) and 50 mL of an aqueous solution of 1 g of PMGD-NH_2 were added into a 250 mL one-necked flask. The flask was sealed, and the mixture was stirred with a magnetic stirrer at 40 °C. After 48 h, the resulting microspheres were precipitated by centrifugation (1.2×10^4 rpm for 10 min) and washed through two cycles of centrifugation/methanol and centrifugation/deionized water.

The amidation of the terminal ester groups was carried out as follows: 50 mL of the methanol solution of EDA (large excess of the terminal group) and 50 mL of the aqueous solution of microspheres obtained after the Michael addition were added into a 250 mL one-necked flask. The flask was sealed, and the mixture was stirred with a magnetic stirrer at 40 °C. After 48 h, the resulting microspheres were precipitated by centrifugation (1.2×10^4 rpm for 10 min) and washed through two cycles of centrifugation/methanol and centrifugation/deionized water.

Both reactions were repeated for a certain number of cycles. Each product was thoroughly washed through two cycles of centrifugation/methanol and centrifugation/deionized water. Finally, the dendritic PAMAM-modified particles could be synthesized.

2.5. Preparation of Fluorescent Polymer Microspheres. Fluorescent and magnetic microspheres could be obtained by the reaction between the isosulfocyanic group of FITC and the amino groups of the dendritic PAMAM-modified magnetic microspheres. In a typical procedure, 10 mL of the ethanol solution of FITC (large excess of the amino groups) was added to a 50 mL one-necked flask that contained 10 mL of the aqueous solution of 0.2 g of magnetic particles grafted by fifth generation PAMAM. After 24 h of stirring in the dark at room temperature, the products were washed through four cycles of centrifugation/ethanol and centrifugation/deionized water.

2.6. Characterization. The IR spectra were recorded on a Nicolet Magna 550 Fourier transform infrared (FTIR) spectrometer. The shapes and sizes of the copolymer particles were recorded on a Philips XL30 scanning electron microscope. Transmission electron microscopy (TEM) images were obtained on a Hitachi H-600 transmission electron microscope by placing one drop of the samples on copper grids coated with carbon. Thermogravimetric analysis (TGA) was performed on a Pyris 1 thermogravimetric analyzer under a flowing nitrogen atmosphere; the scan rate was 10 °C/min, and the temperature range was from 100 to 800 °C. Fluorescence measurements (steady-state) were carried out on an Edinburgh Instruments FLS920 spectrophotometer using a quartz cell. The excitation wavelength was 450 nm. Elemental analyses (EA) of C, H, and N were obtained using a Vario EL III elemental analysis system. The magnetic properties of functional particles were obtained by a vibrating-sample magnetometer (VSM, EG&G Princeton Applied Research VSM, Model 155).

3. Results and Discussion

3.1. Synthesis of Magnetic Poly(MMA-DVB-GMA) Latexes. Over the past few decades, a number of dendrimers have been prepared on solid supports to provide solutions to many problems associated with dendrimer preparation and, particularly, time-consuming purifications using orthodox solution chemistry. On the other hand, the modification of dendrimers for the solid supports also provides a high density of terminal groups as reactive sites for potential applications. In practice, for the immobilization of dendrimers via covalent attachment to the solid supports, an intermediate coupling layer is normally required. For example, PAMAM dendrimers were synthesized by repeating two processes: (1) Michael addition of MA to ammonia as an initiator core and (2) amidation of the resulting ester moieties with EDA. Thus, almost all immobilization of PAMAM dendrimers requires functionalization of amino groups on the surface of the solid supports as a prerequisite. In the case of magnetic particles as the initiator cores, it is well-reported that the magnetite or silica-coated magnetic particles were modified by silicate coupling agents for introducing the amino groups (initiator sites).[15,19] Although a significant reduction in particle size can be achieved to provide the surface area required, too small a particle may not carry enough magnetite and, in practice, would cease to be magnetic. In addition, the nonuniform size and size distribution made it difficult to obtain homogeneous PAMAM dendrimers around the magnetic cores. Therefore, the choice of the right magnetic support is the first challenge. Fortunately, magnetic polymer latexes can fulfill certain criteria as initiator cores for the immobilization of PAMAM to their surface, which have the following properties: (1) larger latex particles with diameters ranging from the submicro- to micrometer, (2) narrow size distribution allowing homogeneous particle behavior, (3) easy surface functionality for covalent grafting, (4) high magnetic content for rapid separation under a magnetic field, and (5) encapsulation of the magnetic material by a inert polymeric matrix to avoid the corrosion of nanoparticles under different chemical environments. However, there have been no reports thus far with regard for the preparation of PAMAM-immobilized magnetic polymer latexes.

Herein, among the various interesting approaches for the elaboration of magnetic latexes, ranging from classical heterogeneous polymerization processes[21−23] to some multistep synthesis procedures,[24−26] we adopted soap-free emulsion and subsequent seed polymerization to prepare magnetic polymer latexes with a narrow size distribution and surface functional groups. This is not only to introduce the amino groups and to improve the homogeneous properties but also to have a core−shell structure in favor of the protection of iron oxides during PAMAM immobilization. According to previous reports,[27,28] first, surfactant-stabilized magnetite nanoparticles were synthesized in a two-step procedure. In the first step, Fe_3O_4 nanoparticles were produced by chemical coprecipitation from an aqueous solution of Fe (II) and Fe (III) chloride in the presence of OA. Then, following the removal of excess primary OA, the particles were coated with a secondary OA layer to form self-organized bilayers on the magnetite nanoparticle surfaces. Figure

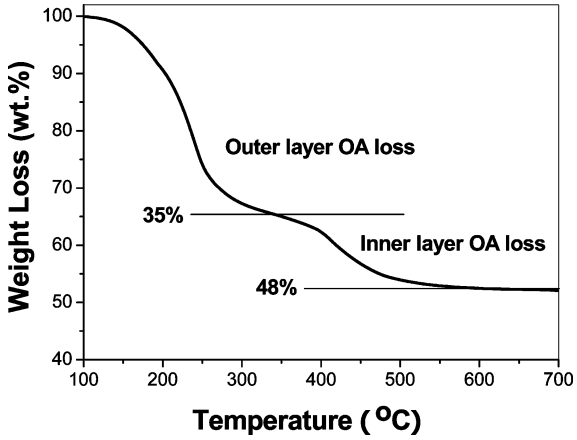

Figure 1. TGA curves of bilayer OA-coated magnetic nanoparticles.

1 presents typical TGA curves for magnetic particles coated with bilayer surfactants. The mass profile exhibited two well-defined decreasing steps. The first mass loss was about 35%, and correspondingly, the inflection temperature was 239 °C, where the mass loss rate was a maximum. The second mass loss was only 13%, and a higher inflection temperature was obtained, about 411 °C. Apparently, for bilayer surfactant-coated particles, the weight reductions for the first and second steps should be attributed to quantitative mass losses of the outer and inner layers of the coating, respectively. The inner OA layers around the magnetite nanoparticles provide an effective means to keep the particles apart during the crystal growth process. Correspondingly, the second mass loss differed only slightly from a previous report.[28] The outer OA layers provided the water solubility for the monolayer-coated Fe_3O_4 nanoparticles on the basis of self-assembly of the long chain moieties of OA. However, a larger mass loss occurred than before.[27,28] The mass loss may be due to the different molecular weights of the surfactants used, leading to an increase of the first mass loss. Additionally, the inner layer has a stronger interaction for the chemisorption of OA molecules on the magnetic particles than the van der Waals attraction between two OA layers. As such, much stronger chemical interactions would be responsible for the higher inflection temperatures of the second mass loss.

For obtaining magnetic polymer microspheres with a uniform size and high content of surface functional groups, first we polymerized MMA monomers to encapsulate the bilayer-OA-stabilized magnetite nanoparticles via the soap-free emulsion route. As shown in Figure 2A, the TEM image presents well-defined magnetic PMMA microspheres with a diameter of ca. 100 nm. However, these magnetic particles exhibited a phase-separated structure observed from the encapsulated magnetite particles beside the spheres. Analogous to this finding, Elaïssari et al. also reported the preparation of polystyrene/Fe_2O_3 composite particles with asymmetric structures, which were due to the phase separation between polystyrene and inorganic magnetic phase.[22] Herein, although there was no hemisphere-type structure based on the thermodynamic incompatibility between the two phases, the presence of heterogeneous encapsulation of the magnetic nanoparticles demonstrated a significant polar difference between PMMA and OA-capped Fe_3O_4 aggregates, particularly in the case of a large amount of OA molecules being present in a composite microsphere. For obtaining a core−shell-like morphology, we envisaged copolymerizing MMA with DVB to rapidly cross-link the PMMA phase inside the particles for further inhibiting the PMMA chain mobility and then preventing partial phase separation. Polymerizations were carried out with 10 wt % DVB with respect to the total amount of the monomers using KPS as the initiator in water. As shown in Figure 2B, the TEM image exhibits the homogeneous encapsulation of Fe_3O_4 nanoparticles within the cross-linked PMMA polymer matrices. The utility of DVB drastically reduces the secondary nucleation due to the higher reactivity than that of MMA monomers. However, from the TEM image, it was observed that the as-prepared magnetic PMMA microspheres with a 10 wt % cross-linking density did not have uniform magnetic contents. Principally, a small amount of MMA monomers may prefer swelling the bilayer-OA-stabilized magnetite to produce the micelles, leading to the formation of magnetic PMMA microspheres with uniform-encapsulated Fe_3O_4 nanoparticles. Herein, it highly is suspected that the used amount of MMA monomers may destroy the surfactants' bilayer structure and thus lead to the coagulation of Fe_3O_4 nanoparticles before polymerization. Thus, the population of the self-nucleation particles increased as well. As a result, with the help of the applied magnetic field, the cross-linked magnetic PMMA microspheres with uniform magnetic properties were separated out of the resulting products and were set as seeds for the polymerization of GMA to introduce the surface functional groups. As shown in Figure 2C, the PGMA shells clearly were observed to coat the magnetic PMMA particles in the continuous seeded polymerization of GMA monomers. Furthermore, these magnetic composite microspheres with a diameter of ca. 200 nm have a more uniform size distribution than the magnetic PMMA seeds observed from the SEM image in Figure 2D. Thus, preformed magnetic poly(MMA-DVB-GMA) composite microspheres may be in favor of the formation of dendritic PAMAM with homogeneous behavior because of their monodisperse size, uniform magnetic properties, and surface functional groups.

3.2. Immobilization of PAMAM Shells to Magnetic Microsphere Surface. In previous work, as mentioned before, dendritic PAMAM was grafted onto solid support surfaces by the repetition of the two processes as shown in Scheme 2. First, EDA was used to react with the epoxy groups on the PGMA shells to produce amino groups for the subsequent Michael addition of MA. Second, the two repeating reactions were carried out involving (1) Michael addition of MA to amino groups as an initiator site introduced onto the magnetic microsphere surface and (2) terminal amidation of the resulting esters with EDA. The treatment of MA and EDA was repeated *n* times to obtain dendrimers (*n*th generation) as shown in the theoretical Scheme 2.

Table 1 shows the amino group content of magnetic polymer latexes after the grafting reaction. The amount of amino groups of the resulting composite particles increased with an increase in the number of generations. Theoretically, the amine number doubled with every generation starting with the amino group initiators. However, the amount of amino groups at every generation increased less than twice from G1 to G5, suggesting that theoretical propagation of PAMAM from the surface was hardly achieved. Such incomplete propagation of dendrimers from amino groups on the surface of magnetic composite particles may be due to the fact that (1) complete Michael addition and the amidation with surface functional groups hardly proceeded because of the heterogeneous reaction system and (2) the grafted chains on the particle surface interfere with the propagation of the dendrimer from the surface because of steric hindrance.

The dendrimer modification process was proven by comparison of FTIR spectra of the different generations of dendritic PAMAM-modified magnetic composite particles as shown in

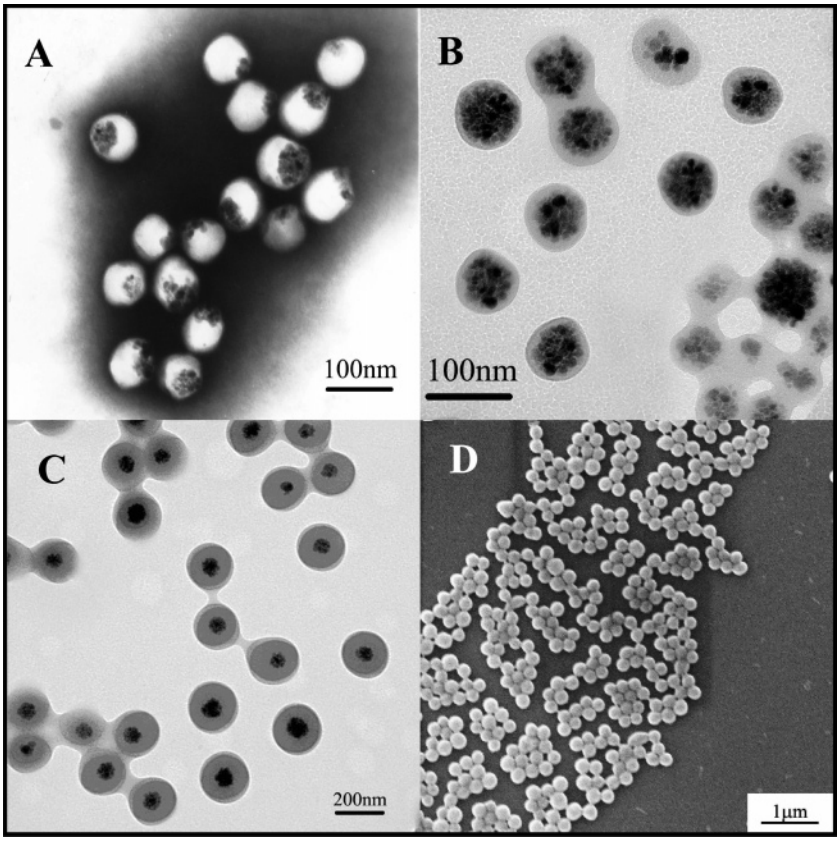

Figure 2. TEM images of the magnetic PMMA polymer microspheres coating the bilayer-OA-stabilized magnetite nanoparticles (A), the magnetic PMMA microspheres with 10 wt % DVB (B), and the magnetic poly(MMA-DVB-GMA) microspheres with DVB of 10 wt % (C). SEM images show magnetic poly(MMA-DVB-GMA) microspheres (D), corresponding to the TEM image in panel C. In panel A, the background was stained by a phosphotungstic acid solution.

Figure 3. It can be seen from Figure 3 that the characteristic peaks at ~1550 and ~1650 cm^{-1} of PAMAM for −C(═O)−NH− are very clear, implying that the dendrimer PAMAM was grafted from the core particles successfully. With the increase of the generation, both characteristic peaks at ~1550 and ~1650 cm^{-1} of PAMAM became stronger and stronger (from G0 to G5). All of these facts reveal the existence of PAMAM dendrimers on the magnetic support surface.

3.3. Magnetic Properties of PAMAM-Grafted Magnetic Composite Microspheres. Magnetic measurements of dendritic PAMAM-grafted magnetic poly(MMA-DVB-GMA) microspheres were carried out using a VSM. As shown in Figure 4, the saturation magnetic moments of these particles reached ca. 4.9 emu/g. This saturation magnetization value was far less than the reference value for the pure magnetite nanoparticles (67.8 emu/g).[29] This can be explained by considering the presence of the thicker shells, leading to a weakening of the magnetic moment. In addition, the magnetic polymer microspheres showed superparamagnetic properties at 305 K indicated by the inset in Figure 4 and exhibited no remanence effect from the hysteresis loops at a low applied magnetic field. These magnetic properties are critical in the applications of biomedical and bioengineering fields. When the microspheres undergo strong magnetization, the efficient magnetic separation is allowed for, and when the applied magnetic field is removed, redispersion of these microspheres will take place rapidly due to a few remnant magnetisms.

3.4. Fluorescence Properties of FITC-Coupled PAMAM Shells. The application of PAMAM dendrimers for cancer treatment has great potential and is under critical investigation, as these macromolecules serve as targeted drug carriers, delivery agents, and imaging agents in human systems.[30] In this way, the multifunctionality and biocompatibility of dendrimer-based particles are crucial for the development of various biomedical technologies. Thus, because of the tertiary amino groups present in the interior of the structure and the primary amino groups present on the surface, the conjugation of functional molecules with the terminal groups may facilitate the integration of novel functions into one single ensemble. Herein, the prepared PAMAM-grafted magnetic polymer microspheres have already fulfilled some requirements of multifunctionalization including targeted delivery via the applied magnetic field, drug loading on the pH-dependent PAMAM shells, and self-fluorescence of dendritic PAMAM for imaging and tracing. However, ideal luminescence properties of the multifunctional microspheres have not been achieved. To date, although some groups have reported the improvement of fluorescence intensity under acidic conditions for the different kinds of dendrimers particularly in the case of the NH_2-terminated PAMAM,[31] the fluorescence emitted is very weak and restricted with a detectable limit. Therefore, the fluorescence probes with functional groups should be attached to the PAMAM shells of the multifunctional microspheres for obtaining excellent imaging functions.

FITC is a popular fluorescence dye, in which the isothiocyanate groups can easily react with amino groups. Thus, via conjugation between terminal amino groups of PAMAM and FITC, the fluorescence probes may be covalently bonded to the surface of the functional microspheres, resulting in the formation of dendritic FITC-terminated PAMAM-modified magnetic poly(MMA-DVB-GMA) microspheres. The photoluminescence properties of microspheres were characterized by fluorescence spectrometry as shown in Figure 5. It was observed that the

SCHEME 2: Theoretical Illustration of Propagation of PAMAM Dendrimer Grafted to Magnetic Poly(MMA-DVB-GMA) Microspheres

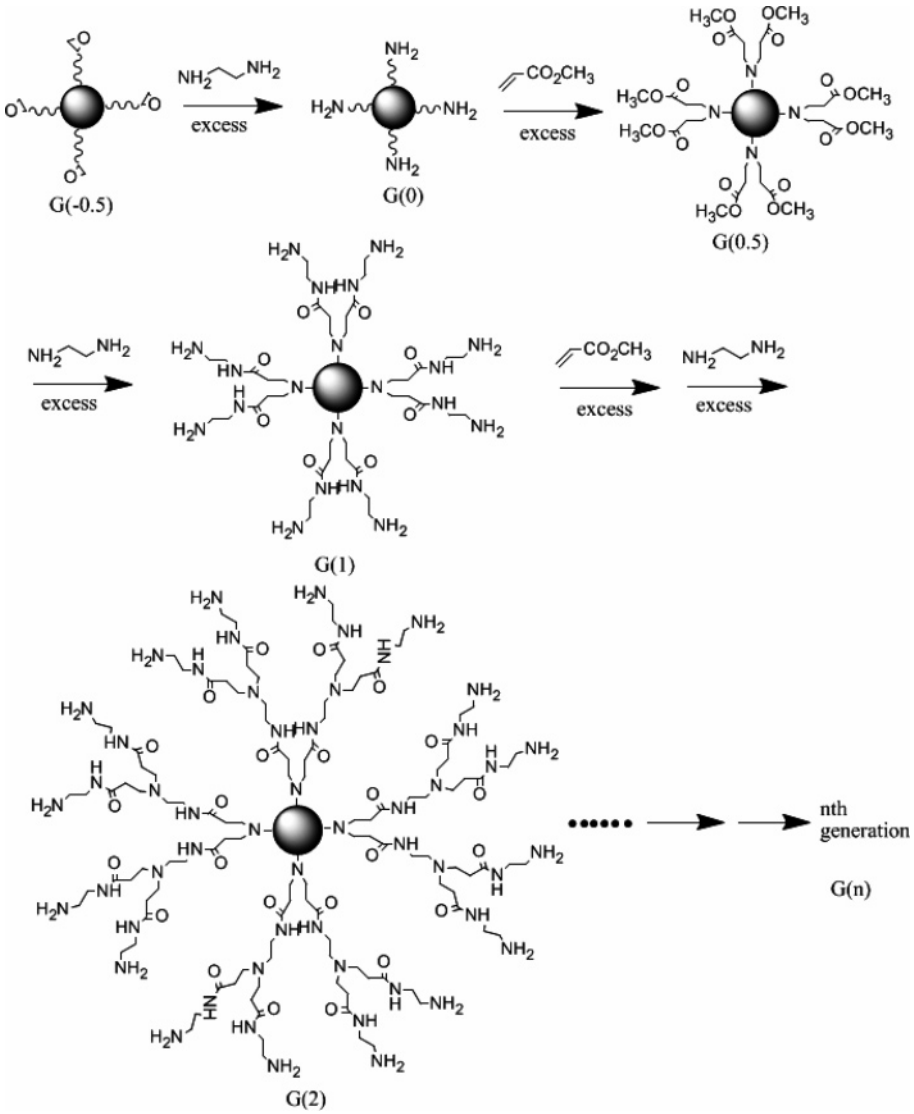

TABLE 1: Amount of Amino Groups on Dendritic PAMAM-Immobilized Magnetic Polymer Latexes via Elemental Analysis

generation	N content (wt %)	C content (wt %)	amino groups (mmol/g)
(−0.5)	0.017	61.29	
G(0)	1.276	59.42	0.456
G(1)	1.795	58.50	0.513
G(2)	2.493	58.17	0.548
G(3)	3.632	57.23	0.716
G(4)	4.037	57.51	0.756
G(5)	5.551	55.51	1.015

peak position of fluorescence emission for the multifunctional microspheres was about 528 nm, a red shift of 13 nm as compared to the free FITC in water (515 nm). It was probably caused by energy transfer from the neighboring FITC molecules attaching to the G5 NH_2-terminated PAMAM. Also, due to the reaction between amino groups and FITC, the resultant products had much narrower peak widths than that of the free FITC in water. The well-stabilized dispersion after FITC coupling, even after storage for several weeks, still retained a strong fluorescence intensity.

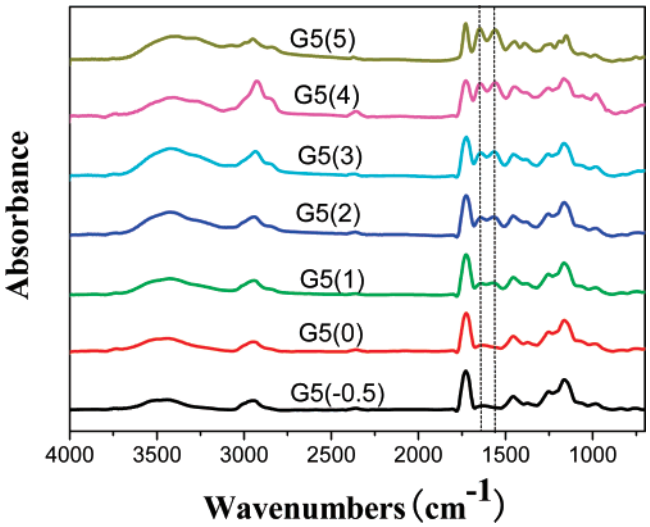

Figure 3. FT-IR spectra of dendritic PAMAM-grafted magnetic composite particles from G(−0.5) to G5.

4. Conclusion

We presented a robust approach to synthesize magnetic polymeric microspheres with immobilization of dendritic PAM-

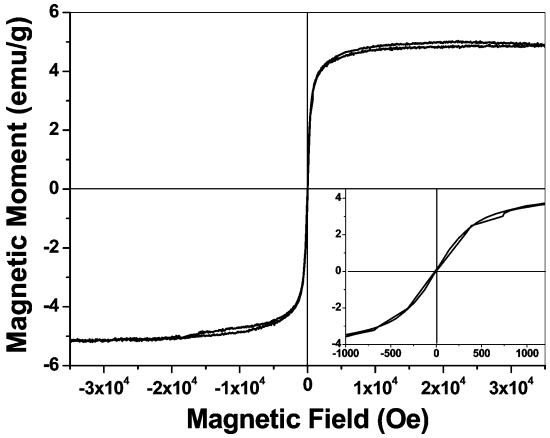

Figure 4. Magnetization curve of G5 PAMAM-immobilized magnetic poly(MMA-DVB-GMA) microspheres at 305 K. Inset is a magnified view of the magnetization curves at low applied fields.

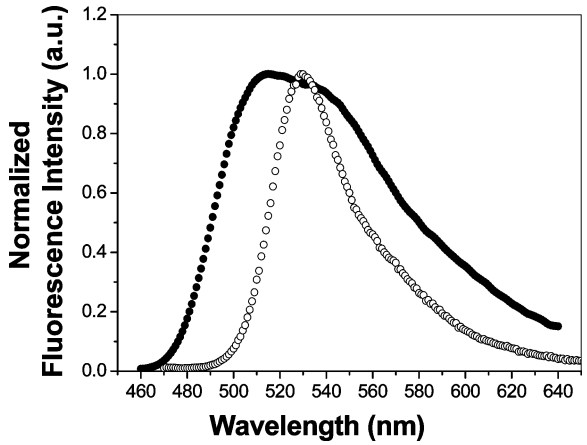

Figure 5. Photoluminescence spectra of the free FITC molecules in water (●) and dendritic PAMAM-grafted magnetic composite microspheres dispersed in aqueous solution (○).

AM shells. First, in the presence of bilayer-OA-coated Fe_3O_4 nanoparticles, the magnetic poly(MMA-DVB) microspheres were prepared via soap-free emulsion polymerization, forming a uniform size and size distribution as well as the well-encapsulated high content of Fe_3O_4 nanoparticles. Herein, the cross-linking agents (DVB) were used to restrict the phase separation between the polymer matrices and the OA-capped Fe_3O_4 nanoparticles. However, a large amount of MMA monomers destroyed the bilayer structures of OA around the Fe_3O_4 nanoparticles, which led to secondary nucleation and nonuniform magnetic content from the aggregates of the lost OA nanoparticles. As such, the applied magnetic field was manipulated to collect the magnetic PMMA seeds for the subsequent polymerization of GMA by seeded polymerization. The PGMA shells homogeneously coated the magnetic PMMA particles well, resulting in the formation of magnetic poly-(MMA-DVB-GMA) microspheres with monodispersity, uniform magnetic properties, and surface terminal $-NH_2$ groups obtained from the reaction of epoxy groups and EDA. The immobilization of the dendritic PAMAM was based on the Michael addition of MA and the amidation of the resulting ester with large excesses of EDA, leading to each successive generation. Although the amount of amino groups from every generation was far less than the theoretical amount, the abundant terminal groups still provided a possibility for the further functionalization of microspheres. FITC molecules were coupled with the terminal $-NH_2$ groups from the PAMAM shells onto the magnetic microspheres. As such, these multifunctional microspheres with well-defined core−shell structures showed pH-triggered drug delivery from the PAMAM shell and photoluminescence and magnetic properties, which could open the door to a new generation of PAMAM-based multifunctional microspheres. Most importantly, a large amount of surface functional groups from the PAMAM shells will allow coupling of a wide variety of functional materials, suggesting that the flexible functional integration strategy will attract much interest in the whole range of potential chemical applications.

Acknowledgment. This work was supported by the National Natural Science Foundation of China (Grants 20728404 and 20674009), the National Science Fund for Distinguished Young Scholars of China (50525310), the Cultivation Fund of the Key Scientific and Technical Innovation Project, Ministry of Education of China (707023), and the Shanghai Leading Academic Discipline Project (B113).

References and Notes

(1) Mornet, S.; Vaseur, S.; Grasset, F.; Verveka, P.; Goglio, G.; Demourgues, A.; Portier, J.; Pollert, E.; Duguet, E. *Prog. Solid State Chem.* **2006**, *34*, 237.
(2) Gupta, A. K.; Curtis, A. S. G. *J. Mater. Sci.: Mater. Med.* **2004**, *15*, 493.
(3) Plank, C.; Schillinger, U.; Scherer, F.; Bergemann, C.; Rémy, J.-S.; Krötz, F.; Anton, M.; Lausier, J.; Rosenecker, J. *Biol. Chem.* **2003**, *384*, 737.
(4) Gupta, A. K.; Gupta, M. *Biomaterials* **2005**, *26*, 3995.
(5) Kohler, N.; Sun, C.; Fichtenholtz, A.; Gunn, J.; Fang, C.; Zhang, M. Q. *Small* **2006**, *2*, 785.
(6) Jordan, A.; Scholz, R.; Wust, P.; Schirra, H. *J. Magn. Magn. Mater.* **1999**, *194*, 185.
(7) Berry, C. C.; Curtis, A. S. G. *J. Phys. D: Appl. Phys.* **2003**, *36*, 198.
(8) Lu, A.-H.; Salabas, E. L.; Schüth, F. *Angew. Chem., Int. Ed.* **2007**, *46*, 1222.
(9) Khng, H. P.; Cunliffe, D.; Davies, S.; Turner, N. A.; Vulfson, E. N. *Biotechnol. Bioeng.* **1998**, *60*, 419.
(10) Ma, Z. Y.; Guan, Y. P.; Liu, H. Z. *J. Polym. Sci., Part A: Polym. Chem.* **2005**, *43*, 3433.
(11) Merrifield, R. B. *J. Am. Chem. Soc.* **1963**, *85*, 2149.
(12) Mitchell, A. R.; Erichson, B. W.; Ryabtsev, M. N.; Hodges, R. S.; Merrifield, R. B. *J. Am. Chem. Soc.* **1976**, *98*, 7357.
(13) Swali, V.; Wells, N. J.; Langley, G. J.; Bradley, M. *J. Org. Chem.* **1997**, *62*, 4902.
(14) Wells, N. J.; Basso, A.; Bradley, M. *Biopolymers* **1998**, *47*, 381.
(15) Pan, B.-F.; Gao, F.; Gu, H.-C. *J. Colloid Interface Sci.* **2005**, *284*, 1.
(16) Tsubokawa, N.; Satoh, T.; Murota, M.; Sato, S.; Shimizu, H. *Polym. Adv. Technol.* **2001**, *12*, 596.
(17) Antebi, S.; Arya, P.; Manzer, L. E.; Alper, H. *J. Org. Chem.* **2002**, *67*, 6623.
(18) Reynhardt, J. P. K.; Yang, Y.; Sayari, A.; Alper, H. *Chem. Mater.* **2004**, *16*, 4095.
(19) Abu-Reziq, R.; Alper, H.; Wang, D. S.; Post, M. L. *J. Am. Chem. Soc.* **2006**, *128*, 5279.
(20) Gao, F.; Pan, B.-F.; Zheng, W.-M.; Ao, L.-M.; Gu, H.-C. *J. Magn. Magn. Mater.* **2005**, *293*, 48.
(21) Xu, H.; Cui, L. L.; Tong, N. H.; Gu, H. C. *J. Am. Chem. Soc.* **2006**, *128*, 15582.
(22) Montagne, F.; Mondain-Monval, O.; Pichot, C.; Elaïssari, A. *J. Polym. Sci., Part A: Polym. Chem.* **2006**, *44*, 2642.
(23) Nunes, J. S.; de Vasconcelos, C. L.; Cabral, F. A. O.; de Araújo, J. H.; Pereira, M. R.; Fonseca, J. L. C. *Polymer* **2006**, *47*, 7646.
(24) Sauzedde, F.; Elaïssari, A.; Pichot, C. *Colloid Polym. Sci.* **1999**, *277*, 846.
(25) Sauzedde, F.; Elaïssari, A.; Pichot, C. *Colloid Polym. Sci.* **1999**, *277*, 1041.
(26) Lansalot, M.; Sabor, M.; Elaïssari, A.; Pichot, C. *Colloid Polym. Sci.* **2005**, *283*, 1267.
(27) Shen, L.; Laibinis, P. E.; Hatton, T. A. *Langmuir* **1999**, *15*, 447.
(28) Wang, P.-C.; Chiu, W.-Y.; Lee, C.-F.; Young, T.-H. *J. Polym. Sci., Part A: Polym. Chem.* **2004**, *42*, 5695.
(29) Panda, R. N.; Gajbhiye, N. S.; Balaji, G. *J. Alloys Compd.* **2001**, *326*, 50.
(30) Stitibara, S. E.; Frey, H.; Haag, R. *Angew. Chem., Int. Ed.* **2004**, *41*, 1329.
(31) Wang, D.; Imae, T. *J. Am. Chem. Soc.* **2004**, *126*, 13204.